



A model of vegetated exterior facades for evaluation of wall thermal performance



Irina Susorova^{a,*}, Melissa Angulo^{b,c}, Payam Bahrami^b, Brent Stephens^c

^a College of Architecture, Illinois Institute of Technology, 3300 S. Federal St., Chicago, IL 60616, USA

^b Council on Tall Buildings and Urban Habitat (CTBUH), Illinois Institute of Technology, 3360 S. State St., Chicago, IL 60616, USA

^c Department of Civil, Architectural and Environmental Engineering, Illinois Institute of Technology, 3201 S. Dearborn Street, Chicago, IL 60616, USA

ARTICLE INFO

Article history:

Received 27 February 2013

Received in revised form

15 April 2013

Accepted 23 April 2013

Keywords:

Green facades

Facade vegetation

Facade thermal performance

Vegetation models

Energy efficient

Buildings

ABSTRACT

A mathematical model of an exterior wall covered with climbing vegetation has been developed to evaluate the thermal effects of plants on heat transfer through building facades. This model allows for analysis of how various plant physiological parameters such as leaf area index, average leaf dimension, and leaf absorptivity can improve facade thermal performance by reducing the exterior wall surface temperatures and heat flux through the facade. The model has been verified with a set of experiments that measured both bare and vegetated facade thermal performance of an educational building in Chicago, IL, during the summer. A sensitivity analysis was also conducted to elucidate the relative impacts of plant characteristics, weather conditions, climate zones, wall assembly types, and facade orientation on vegetated facade thermal performance. Overall, results herein show that a plant layer added to the facade can improve its effective thermal resistance by 0.0–0.7 m² K/W, depending on a range of inputs for wall parameters, climate zones, and plant characteristics (particularly leaf area index). These improvements are especially pronounced in predominantly warm climates with high solar radiation and, to a lesser extent, low wind speeds. The model developed herein can ultimately be used both to assess facade thermal improvements in existing buildings retrofitted with green walls and to design green walls for optimal energy efficiency in new construction.

© 2013 Elsevier Ltd. All rights reserved.

1. Introduction

In recent years, designers have promoted the idea of integrating plants into the envelopes of buildings to address both aesthetic and energy concerns. Such vegetated walls traditionally include vines or bushes growing directly along the facade or along trellises and wire supports. More complex vegetated wall types also include a layer of soil and are integrated directly into the facade construction. In terms of energy performance, plants on walls can be used to lower both (i) surrounding air temperatures (reducing the heat island effect) and (ii) facade surface temperatures immediately behind the vegetation, which can reduce conductive heat transfer through building envelopes and thereby reduce cooling loads.

Several previous studies have demonstrated these effects. For example, early experiments measuring the thermal effects of climbing plants on building facades in summer demonstrated a 1–3 °C reduction in the ambient air temperature near a vegetated

facade [1]. Reported reductions in facade surface temperatures immediately behind vegetation have ranged from 8.2 °C [2] to 1.9–8.3 °C [3], depending primarily on the density of the plant layer. In a study evaluating the thermal effects of nine types of green wall systems, Wong et al. [4] measured a reduction of 3.3 °C in ambient air temperature, which corresponded to a 1.1–11.6 °C decrease in the facade surface temperature immediately behind the vegetation, depending on vegetation type. Two more recent studies on other vegetated walls demonstrated a reduction in facade surface temperatures behind vegetation of 5.5 °C [5] and 1.2–3.9 °C [6].

These reductions in facade surface temperatures behind vegetation have also been shown to lead to reductions in energy use. For example, Di and Wang [2] measured a 28% reduction in the peak-cooling load through a west-facing wall of a building covered with thick ivy on a clear summer day. Although these and other previous studies have demonstrated that a variety of green wall types can reduce cooling loads in some climates and conditions, most previous vegetated wall experimental investigations have been limited to evaluating the effects of a particularly narrow range of plants. Additionally, results are typically valid only for the particular settings of the experiments and typically over a short

* Corresponding author. Tel.: +1 312 882 0632.

E-mail addresses: irinasusorova@gmail.com, isusorov@hawk.iit.edu (I. Susorova).

Nomenclature			
c_{pair}	specific heat of air at constant pressure (29.3 J/mol °C)	R_{plant}	effective thermal resistance of the plant layer (m ² K/W)
c_{pwall}	specific heat of wall material (J/kg K)	RH	relative humidity
$C_{\text{bw}}, C_{\text{vw}}$	convection to/from the bare facade and vegetated facade (W/m ²)	$S_{\text{bw}}, S_{\text{vw}}$	heat stored in the wall material of the bare and vegetated facades (W/m ²)
D	leaf characteristic dimension (m)	$SR_{\text{bw}}, SR_{\text{vw}}$	shortwave radiation to/from the bare facade and vegetated facade (W/m ²)
e_a	partial water vapor pressure of air (kPa)	t	time (s)
$e_{s(T)}$	water vapor pressure of air at saturation (kPa)	T_{air}	air temperature (K)
$F_{\text{gr}}, F_{\text{sky}}$	view factors to the ground and to the sky	T_{dewpoint}	dewpoint temperature (K)
$g_{\text{asll}}, g_{\text{asul}}$	actual stomatal conductance of the lower and upper leaf surface (mol/m ² s)	T_{gr}	ground temperature (K)
g_{bh}	boundary layer conductance for heat transfer (mol/m ² s)	T_{in}	air temperature of the room interior (K)
g_{bv}	boundary layer conductance for vapor (mol/m ² s)	$T_{\text{inbw}}, T_{\text{invw}}$	measured interior surface temperature of the bare and vegetated facade (K)
g_c	convective conductance (mol/m ² s)	T_{leaf}	temperature of the leaf surface (K)
g_r	radiative conductance (mol/m ² s)	T_{sky}	clear sky temperature (K)
$g_{\text{sll}}, g_{\text{sul}}$	typical stomatal conductance of the lower and upper leaf surface (mol/m ² s)	$T_{\text{sbw}}, T_{\text{svw}}$	exterior surface temperature of the bare and vegetated facade (K)
g_v	vapor conductance (mol/m ² s)	V_{air}	wind speed (m/s)
$h_{\text{bw}}, h_{\text{vw}}$	convection heat transfer coefficient of the bare and vegetated facade surface (W/m ² K)	XR	radiative exchange between the bare facade and the plant layer (W/m ²)
I_{max}	maximum total solar radiation incident on a surface (W/m ²)	α_{wall}	facade absorptivity for solar radiation
I_t	total solar radiation incident on a surface (W/m ²)	α_{leaf}	leaf absorptivity for solar radiation
k	material conductivity (W/m K)	γ	thermodynamic phsycometer constant (0.000666 1/°C)
L	wall thickness (m)	γ'	apparent phsycometer constant (1/°C)
LAI	leaf area index	Δ	slope of the saturation vapor pressure function (kPa/°C)
$LR_{\text{bw}}, LR_{\text{vw}}$	longwave radiation to/from the bare facade and vegetated facade (W/m ²)	ϵ_{leaf}	leaf emissivity of longwave radiation
P_{air}	atmospheric pressure at sea level (100 kPa)	ϵ_{wall}	facade surface emissivity of longwave radiation
$Q_{\text{bw}}, Q_{\text{vw}}$	total heat flux through the wall with the bare facade and vegetated facade (W/m ²)	ϵ_{sky}	sky emissivity (approximately 1)
Q_{leaf}	the total radiation absorbed by a vertical layer of plants (W/m ²)	η_{root}	minimum value of soil moisture in the root zone of the plant
$r_{\text{asll}}, r_{\text{asul}}$	actual stomatal resistance of the lower and upper leaf surface (m ² s/mol)	η_{wilt}	level of soil moisture below which permanent wilting of the plant occurs
$r_{\text{sll}}, r_{\text{sul}}$	typical stomatal resistance of the lower and upper leaf surface (m ² s/mol)	κ	attenuation coefficient
$R_{\text{bw}}, R_{\text{vw}}$	effective thermal resistance of the bare facade and vegetated facade (m ² K/W)	ρ	wall material density (kg/m ³)
		λ	latent heat of vaporization of water (kJ/kg) (2501 kJ/kg at 0 °C)
		σ	Stefan–Boltzmann constant (0.0000005673)
		τ	transmissivity of total radiation through a plant layer
		θ	tilt angle of the facade surface

time period. The purpose of this study is to develop a comprehensive mathematical model of a vegetated wall (without soil) that can be used to evaluate the effects of climbing plants on the thermal performance of a building facade for various input parameters, including weather conditions, climate zones, facade orientation, wall assembly types, and, importantly, a variety of important plant characteristics.

2. Model development

Several previous studies have constructed heat transfer models for thermal analysis of vegetated facades. For example, Holm [7] developed a model to predict thermal improvements in a facade covered with plants for different orientations, climates, and wall construction types. However, this model was based on a particular set of plant characteristics measured in laboratory tests and did not account for plant evapotranspiration. Di and Wang [2] constructed a mathematical model of heat flux through vegetated facades based on experimental investigations to calculate conductive heat transfer and energy use reductions. Kontoleon and Evmorfopoulou [8] built a simplified mathematical model of a vegetated wall using

the thermal resistance analogy to evaluate the effect of facade orientations, leaf density, and insulation layer placement on facade thermal performance and cooling load reductions. These previous studies have relied primarily on plant characteristics measured during individual experiments as model inputs as opposed to computing them directly, which is a focus of this work.

Mathematical models simulating the effect of plants in green roofs were developed by Alexanri [9] and Sailor [10], whose model was also implemented in the EnergyPlus energy analysis software [11]. Both dynamic mathematical models simulated one-dimensional vertical heat flux through a green roof assembly, which included a layer of soil. The heat flux through the horizontal plant layer was simulated using the calculations of vegetation canopy models commonly used in climatology. However, green roof models cannot be directly used to evaluate thermal properties and heat flux through vegetated walls because of the absence of the soil layer and the difference in heat exchange processes.

At present, despite multiple studies on vegetation thermal effects, there are no published models of vegetated walls capable of simulating the effect of plants on the facade thermal performance for variable plant characteristics, facade properties, building

orientations, and weather conditions. Therefore, the model described in this work offers an improvement over previous models by computing plant physiological processes, including evapotranspiration and radiative and convective heat exchange between the plant layer, the facade, the surrounding environment, and the ground and using individual plant characteristics inputs (e.g., leaf absorptivity, typical leaf dimension, leaf area index, radiation attenuation coefficient, and leaf stomatal conductance) and weather data to simulate the impacts of vegetated walls on facade thermal performance. The next section describes the model development in more detail.

2.1. Vegetation model description

The proposed vegetated facade model simulates the one-dimensional heat flux through the depth of a vertical layer of vegetation. The model accounts for short-wave radiative transmission through the plant layer, long-wave radiative exchange between the plant layer and the environment, convective heat transfer to and from vegetation, and evapotranspiration from leaves. The model represents a layer of vertical plants rooted in the ground, such as vines or flat vertical shrubs growing directly against a building exterior wall without the use of soil or substrate. Several model assumptions summarized below were based on common assumptions made in other studies modeling vegetation [9,10,13–17]:

- The model considers plants only during the growing season.
- Leaves are uniformly distributed and oriented in the vegetation layer. Individual leaf angles are not considered.
- Plant parameters including leaf absorptivity, leaf dimension, leaf area index, radiation attenuation coefficient, and plant stomatal conductance are constant and do not change with season.
- For calculating emitted radiation from the plant surface, the temperature of a leaf is assumed to be the same as air temperature.
- Heat flow through a layer of vegetation occurs only horizontally; vertical heat flux is not considered.
- External factors that may vary with height, such as wind speed, are assumed to be constant for the low-rise facades considered.
- The level of soil moisture at plant roots is constant; no precipitation is considered.
- Air beneath stomatal pores is saturated with water.

Most plants can typically survive only within a narrow temperature range between 0 °C and 40 °C [14,15,18]. Therefore, the

plant layer affects the facade thermal performance only during relatively warm weather when the indoor room temperature is lower than the facade exterior surface temperature and heat flux is in the direction from outdoors to indoors. In cold weather, when the direction of the heat flux is reversed from the indoors to outdoors the plant layer has little effect; the model assumes the value of the plant thermal resistance to be zero in cold weather.

The vegetated facade model calculates the effects of plants on the reduction in the facade surface temperature and heat flux through the exterior wall. The model does not account for wind reduction effects because information is lacking on convective heat transfer coefficients at vertical vegetated facade surfaces.

2.2. Facade energy balance and heat flux calculations

Fig. 1 describes the 1-D surface energy balance used in the vegetated wall model.

A building facade receives shortwave radiation SR from the sun (direct, scattered from the sky, and reflected from the ground and atmosphere) and also exchanges longwave thermal radiation LR between the ground, sky, and surrounding surfaces [11,19,20]. Radiation absorbed by the facade is either emitted back into the environment, transferred to or away from the wall by convection to the outdoor air C , or transferred to the building interior by conduction Q , where energy can also be stored in the wall material S . At any moment in time, the energy balance of a bare wall (bw) is thus:

$$SR_{bw} + LR_{bw} + C_{bw} = Q_{bw} + S_{bw} \quad (1)$$

The energy balance of the vegetated wall (vw) includes an additional term (XR) for the radiative exchange between the leaves of the plant layer and the facade surface, as shown in Eq. (2).

$$SR_{vw} + LR_{vw} + XR + C_{vw} = Q_{vw} + S_{vw} \quad (2)$$

The developed model solves the facade energy balance equations with respect to heat flux Q by calculating its components. The facade incident shortwave radiation SR , longwave radiation LR , convective heat flux C , and heat flux to and from the bare and vegetated facades Q are shown in Eqs. (3)–(11).

$$SR_{bw} = I_t \alpha_{wall} \quad (3)$$

$$SR_{vw} = I_t \alpha_{wall} \tau \quad (4)$$

$$LR_{bw} = \epsilon_{wall} \epsilon_{sky} \sigma F_{sky} (T_{sky}^4 - T_{sbw}^4) + \epsilon_{wall} \epsilon_{gr} \sigma F_{gr} (T_{gr}^4 - T_{sbw}^4) \quad (5)$$

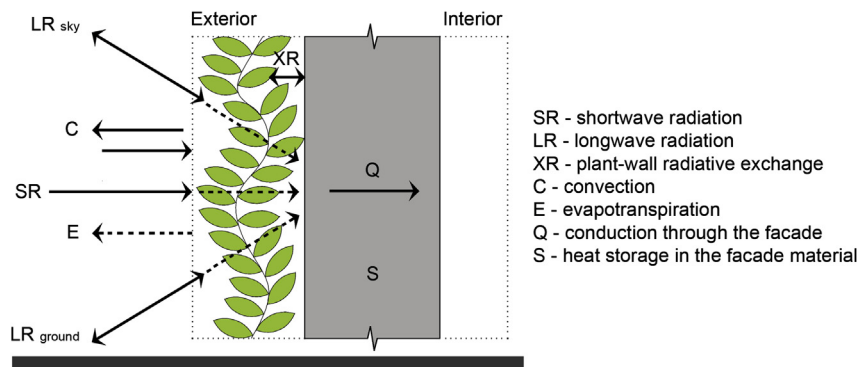


Fig. 1. Energy balance of a vegetated facade.

$$LR_{vw} = \tau \epsilon_{\text{wall}} \epsilon_{\text{sky}} \sigma F_{\text{sky}} (T_{\text{sky}}^4 - T_{\text{svw}}^4) + \tau \epsilon_{\text{wall}} \epsilon_{\text{gr}} \sigma F_{\text{gr}} (T_{\text{gr}}^4 - T_{\text{svw}}^4) \quad (6)$$

$$XR = (1 - \tau) \frac{\epsilon_{\text{leaf}} \epsilon_{\text{wall}} \sigma}{(\epsilon_{\text{leaf}} + \epsilon_{\text{wall}} - \epsilon_{\text{leaf}} \epsilon_{\text{wall}})} (T_{\text{svw}}^4 - T_{\text{leaf}}^4) \quad (7)$$

$$C_{bw} = h_{bw} (T_{\text{air}} - T_{\text{sbw}}) \quad (8)$$

$$C_{vw} = h_{vw} (T_{\text{air}} - T_{\text{svw}}) \quad (9)$$

$$Q_{bw} = \frac{T_{\text{sbw}} - T_{\text{in}}}{R_{bw}} \quad (10)$$

$$Q_{vw} = \frac{T_{\text{svw}} - T_{\text{in}}}{R_{bw}} \quad (11)$$

where I_t is the total solar radiation incident on the facade (W/m^2), α_{wall} is the solar absorptivity of the bare facade (0–1), τ is the transmissivity of radiation through the plant layer (0–1), ϵ_{wall} is the emissivity of the bare facade (0–1), ϵ_{sky} is the sky emissivity (0–1), ϵ_{leaf} is the emissivity of the leaf (0.96), σ is the Stefan–Boltzmann constant ($5.67 \times 10^{-8} \text{ W/m}^2 \text{ K}^4$), F is the view factor between the wall and sky or wall and ground (0–1), T_{sky} is the sky temperature (K), T_{air} is the air temperature (K), T_{sbw} is the bare facade surface temperature (K), T_{svw} is the facade surface temperature behind vegetation (K), T_{leaf} is the leaf temperature (K), h_{bw} is the convection heat transfer coefficient of the bare facade ($\text{W/m}^2 \text{ K}$), h_{vw} is the convection heat transfer coefficient of the vegetated facade ($\text{W/m}^2 \text{ K}$), and T_{in} is the indoor wall surface temperature (K).

The heat absorbed by the facade exterior surface is not necessarily transferred to the interior surface immediately. It is stored in the wall material and later is released into the indoor space with a time delay, which attenuates the heat flux through the wall. This thermal lag effect depends on the heat capacity of the wall material; for example, brick and concrete can store heat up to 6 h, depending on wall thickness, density, and specific heat capacity [21]. Thermal lag can be modeled using wall thermal capacity, which is analogous to a capacitor in an electrical circuit diagram. Thermal energy storage S for bare and vegetated conditions is calculated according to Eqs. (12) and (13) [11,19,20].

$$S_{bw} = L c_{p\text{wall}} \rho \left(\frac{dT_{\text{sbw}}}{dt} \right) \quad (12)$$

$$S_{vw} = L c_{p\text{wall}} \rho \left(\frac{dT_{\text{svw}}}{dt} \right) \quad (13)$$

where L is the wall thickness (m), $c_{p\text{wall}}$ is the specific heat of the wall material (J/kg K), ρ is the wall material density (kg/m^3), and t is the time (s).

The energy balance equations of the bare and vegetated facades are solved for the exterior surface temperature at one-minute time steps in this work. The model advances forward in time computing the current facade surface temperature based on the temperature at the previous time step using a numerical bisection method. The energy balance is calculated using the R statistical software package [22]. The energy balances for the bare and vegetated walls use multiple model input parameters that are either known or computed. Weather parameters are taken from weather data files for different geographic locations available from the U.S. Department of Energy [23]. Plant and facade parameters are taken from

literature on biological ecology and building physics as described in subsequent sections [13–15,24,25].

2.3. Effective thermal resistance of the plant layer

To better summarize the impacts of plant layers on heat conduction through facades (Eqs. (10) and (11)) and to compare results to other insulating materials, we utilize a metric of “effective thermal resistance” of the plant layer in this work. The effective R -value of bare and vegetated facades is calculated as the temperature gradient between the indoor and outdoor surfaces of the material itself divided by the dynamic heat flux through the wall; therefore, it accounts for reductions in conductive heat transfer attributed to the plant layer in terms of an additional resistance. Because we model instantaneous surface temperatures and heat flux through the wall in both bare and vegetated cases, effective R -values can then be calculated under a range of other conditions and varying input parameters, including weather conditions and plant and facade properties. This concept can be illustrated through the analogy of an electric circuit diagram where material thermal resistances are presented as resistors in series (Fig. 2).

Using the equation of the heat flux through the facade one can find the instantaneous effective thermal resistances of the bare facade R_{bw} using Eq. (14).

$$R_{bw} = \frac{T_{\text{sbw}} - T_{\text{in}}}{Q_{bw}} \quad (14)$$

where T_{sbw} is the bare facade exterior surface temperature (K), T_{in} is the indoor surface temperature, and Q_{bw} is the heat flux through the exterior wall (W/m^2). To capture the reduction in heat flux through the exterior wall covered with a plant layer, the instantaneous effective thermal resistance of the vegetated facade R_{vw} is calculated as follows:

$$R_{vw} = R_{bw} \frac{Q_{bw}}{Q_{vw}} = \frac{T_{\text{sbw}} - T_{\text{in}}}{Q_{vw}} \quad (15)$$

where Q_{vw} is the heat flux through the wall with the plant layer (W/m^2). Knowing the effective thermal resistances of the bare and vegetated facades, the instantaneous effective thermal resistance of the plant layer R_{plant} can be estimated using Eq. (16).

$$R_{\text{plant}} = R_{vw} - R_{bw} \quad (16)$$

During mild conditions when the heat fluxes through the facade are minimal, the plant effective R -value calculations are not meaningful. In this case (i.e., $Q < 10 \text{ W/m}^2$), effective plant R -values are considered negligible and set to zero in this work.

2.4. Convective heat transfer coefficient

The convective heat transfer coefficient for the bare facade is calculated with an equation suggested by the EnergyPlus Engineering Ref. [11]

$$h = a + bV + cV^2 \quad (17)$$

where h is the convective surface heat transfer coefficient ($\text{W/m}^2 \text{ K}$), V is the local wind speed (m/s), and a , b , and c are the material roughness coefficients. The model assumes that the facade is made of a material with a medium-rough surface for which the material coefficients are 10.79, 4.192, and 0. Thus, the convective heat coefficient h_{bw} for the bare facade is estimated as:

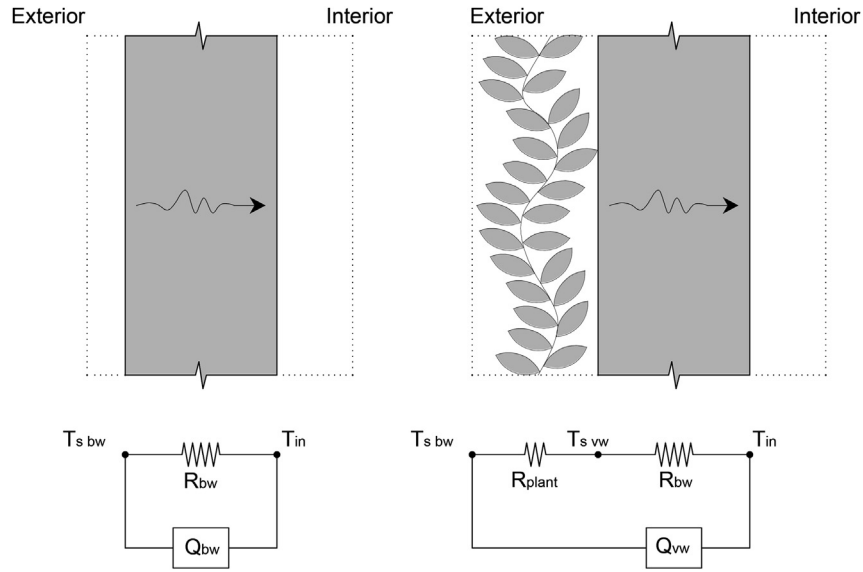


Fig. 2. Heat flux through the bare facade (left) and vegetated facade (right) expressed as an electrical circuit diagram.

$$h_{bw} = 10.79 + 4.192V_{air} \quad (18)$$

where V_{air} is the air speed at the bare facade (m/s). Although some studies showed that vegetation on walls can decrease wind speed at vegetated wall surfaces [6,14], we are not aware of robust studies on decreased values of convective heat transfer coefficients for wide ranges of vegetated facade types. In the absence of better data, the present model assumes $h_{bw} = h_{vw}$. However, this assumption should be explored in future studies.

2.5. Leaf temperature

A typical broad leaf is often represented as a flat thin plate that has radiative and convective heat exchange with the surrounding atmosphere and evaporates water from its surface (conductive heat transfer is insignificant) [15]. Leaf surface temperature is a complex function of multiple factors, such as solar radiation, air humidity, wind speed, and internal leaf carbon dioxide concentration. The leaf surface temperature in the vegetation model is found using the calculations by Campbell [14]

$$T_{leaf} = T_{air} + \frac{\gamma'}{\frac{\Delta}{P_{air}} + \gamma'} \left[\frac{Q_{leaf}}{g_c c_{pair}} - \frac{e_s(T) - e_a}{P_{air} \gamma'} \right] \quad (19)$$

where T_{air} is the air temperature ($^{\circ}\text{C}$); γ' is the apparent psychrometer constant ($1/^{\circ}\text{C}$); Δ is the slope of the saturation vapor pressure function ($\text{kPa}/^{\circ}\text{C}$); P_{air} is the atmospheric pressure at sea level (kPa); Q_{leaf} is the total radiation absorbed by a vertical layer of plants (W/m^2); g_c is the heat conductance ($\text{mol}/\text{m}^2\text{s}$); c_{pair} is the specific heat of air at constant pressure ($\text{J}/\text{mol } ^{\circ}\text{C}$); $e_s(T)$ is the water vapor pressure of the air at saturation (kPa), and e_a is the partial water vapor pressure of the air (kPa). The apparent psychrometer constant is

$$\gamma' = \frac{\gamma g_c}{g_v} \quad (20)$$

where γ is the thermodynamic psychrometer constant and g_v is the vapor conductance through air. The heat conductance through air g_c is

$$g_c = g_r + g_{bh} \quad (21)$$

where g_r is the radiative conductance obtained from tables by Campbell [14] and g_{bh} is the boundary layer conductance for heat transfer through air calculated as

$$g_{bh} = 1.4 \left(0.135 \sqrt{\frac{V_{air}}{D}} \right) \quad (22)$$

where D is the leaf characteristic dimension (m). The vapor conductance through air is

$$g_v = \frac{0.5g_{asul}g_{bv}}{g_{asul} + g_{bv}} + \frac{0.5g_{asll}g_{bv}}{g_{asll} + g_{bv}} \quad (23)$$

where g_{asll} is the actual stomatal conductance of the lower leaf surface; g_{asul} is the actual stomatal conductance of the upper leaf surface, and g_{bv} is the boundary layer conductance for vapor calculated as

$$g_{bv} = 1.4 \left(0.147 \sqrt{\frac{V_{air}}{D}} \right) \quad (24)$$

The slope of the saturation vapor pressure function is given by

$$\Delta = \frac{4217e_s(T)}{(240.97 + T_{air})^2} \quad (25)$$

The total radiation absorbed by a vertical layer of plants Q_{leaf} is calculated as

$$Q_{leaf} = I_t \alpha_{leaf} + \epsilon_{leaf} \sigma F (T_{sky}^4 + T_{gr}^4) - \epsilon_{leaf} \sigma (T_{air})^4 \quad (26)$$

where T_{gr} is the temperature of the ground which is assumed to be the same as the outside air temperature T_{air} . It should be noted that to calculate the radiation emitted by a vertical layer of plants, the air temperature T_{air} was used instead of the leaf temperature T_{leaf} , not yet calculated.

The water vapor pressure of the air at saturation and the partial water vapor pressure of the air are given by

$$e_s(T) = 0.611 \exp \frac{17.502 T_{\text{air}}}{(T_{\text{air}} + 240.97)} \quad (27)$$

$$e_a = e_s(T) RH \quad (28)$$

2.6. Auxiliary calculations

The evaluation of several sky temperature models [19,26,27] showed that the vegetated wall model outputs were not very sensitive to sky temperature. The sky temperature is therefore calculated using a simple relationship from Straube and Burnett [19]

$$T_{\text{sky}} = T_{\text{air}} \left[0.8 + \left(T_{\text{dewpoint}} - 273 \right) / 250 \right]^{0.25} \quad (29)$$

Finally, the view factor F between objects and sources of longwave radiation is the fraction of radiation leaving an object of one shape that is intercepted by an object of similar or different shape [14]. Here, the view factors for the ground and the sky are calculated as [11]

$$F_{\text{gr}} = 0.5(1 - \cos \theta) \quad (30)$$

$$F_{\text{sky}} = 0.5(1 + \cos \theta) \quad (31)$$

where θ is the tilt angle of the facade surface in relation to the ground ($\theta = 90^\circ$ for a vertical facade and $\theta = 0^\circ$ for a roof). For a vertical surface with a tilt angle 90° , both view factors are 0.5.

2.7. Plant parameters

The model uses the following input parameters for plant characteristics.

2.7.1. Leaf absorptivity α_{leaf}

Leaf absorptivity is the fraction of incident solar radiation absorbed by a surface. Leaf absorptivity, which depends on leaf color, leaf texture, and plant age, helps plants to avoid overheating in hot climates and to intercept more radiation in cold climates. Plant features, such as a layer of wax on the leaf surface, leaf pubescence, thorns, and salt crystals, can vary leaf absorptivity. For most deciduous broad leaves, average solar absorptivity is 0.34–0.44 for low sun angles and 0.48–0.56 for high sun angles. The average leaf absorptivity is 0.4–0.6 [14].

2.7.2. Leaf typical dimension D

The leaf typical dimension is the characteristic leaf width of a plant [14]. The leaf characteristic dimension plays an important role in convective heat and vapor conductance between plant leaves and the air.

2.7.3. Leaf area index, LAI

The leaf area index is the total projected area of leaves per unit surface area which can vary from 0.01 for short plants with small leaves, to 3 for leafy shrubs, and to 7 for a dense forest canopy [28].

2.7.4. Radiation attenuation coefficient κ

The radiation attenuation coefficient indicates the decrease in the absorbed radiation in the plant canopy [12]. It varies between 0 and 1 where lower values (0.3–0.5) correspond to vertical leaves with leaf angles less than 45° and higher values (0.7–1) correspond to horizontal leaves with leaf angles more than 45° [18]. When the leaves are perpendicular to the wall, $\kappa = 0$, and when they are parallel to the wall, $\kappa = 1$.

2.7.5. Typical leaf stomatal conductance g_s

Typical leaf stomatal conductance is the rate of water vapor leaving the plant surface through the pores on the leaf surface during transpiration. It depends on the amount of stomatal pores per leaf surface area and the pore size. The reciprocal of conductance, stomatal resistance r_s , is $1/g_s$. Stomatal pores occupy 0.2–2% of the leaf surface and are located on both surfaces of a leaf (amphistomatous leaves) or only on the lower surface (hypostomatous leaves) [25]. Stomatal pores control the gas exchange between a plant and its environment by adjusting the size of pore apertures depending on the plant's needs and external conditions, including the illumination level, air temperature, relative humidity, and solar radiation. Stomatal resistance tends to increase with higher air temperature and lower relative humidity, which is a reaction by plants to conserve moisture [15]. The dependence of stomatal resistance on solar radiation is given by [29]

$$r_{\text{as}} = r_s \left[\frac{I_{\text{max}}}{0.03 I_{\text{max}} + I_t} + \left(\frac{\eta_{\text{wilt}}}{\eta_{\text{root}}} \right)^2 \right] \quad (32)$$

where r_{as} is the actual leaf stomatal resistance, r_s is the typical leaf stomatal resistance, I_{max} is the maximum total solar radiation incident on leaves, I_t is the actual total solar radiation incident on leaves, η_{wilt} is the level of soil moisture below which permanent wilting of the plant occurs (0.39 for peat soil), and η_{root} is the minimum value of soil moisture in the root zone of the plant (assumed to be 0.7).

In plant physiology, it is common to express stomatal conductance in m/s or $\text{mol/m}^2 \text{ s}$ and stomatal resistance in s/m and $\text{m}^2 \text{ s/mol}$; approximate conversion for stomatal resistance at sea level for 25°C is [13]

$$r_s (\text{m}^2 \text{ s/mol}) = 0.025 r_s (\text{s/m}) \quad (33)$$

Typical stomatal conductance values for leaves are 0.002–0.010 m/s (0.08–0.40 $\text{mol/m}^2 \text{ s}$) and stomatal resistance values are 100–500 s/m (2.5–13 $\text{m}^2 \text{ s/mol}$) [15,25].

3. Model verification

3.1. Experiment description

An experiment measuring the performance of vegetation-covered walls was conducted to validate the vegetated facade model. The experiment consisted of measuring the facade thermal performance of a building covered with climbing plants on the campus of the Illinois Institute of Technology. Two exterior areas on the south facade, approximately 5 m from the ground, were selected for the measurements: an area densely covered with plants and an area without plants (Fig. 3). The interior space behind the measured facade is an air-conditioned office space. The experiment was conducted during four days from August 29 until September 1, 2012; the measurements were collected at 1-min time intervals. The weather conditions during the experiment are summarized in Table 1.

The measured building was three stories tall. Its facade had a composite structure of steel I-beam columns spaced 3 m apart that horizontally divided the facade into six sections. Each one-story section had metal frame windows occupying approximately 70% of the area and brick infills occupying the remaining 30%. The following parameters were measured at individual points during the experiment:



Fig. 3. South facade of Siegel Hall on the campus of the Illinois Institute of Technology (left) and the instruments measuring two facade areas (right).

- Outdoor air temperature
- Surface temperatures of the bare facade
- Surface temperature of the vegetated facade behind the plants
- Surface temperature of the leaf surface
- Surface temperature of the interior wall behind the bare and vegetated facades
- Air temperature within the vegetation layer 5 cm from the facade
- Relative humidity
- Wind speed near the facade
- Total horizontal solar radiation

The outdoor air temperature and relative humidity were measured 30 cm from the facade using an Extech RHT20 humidity and temperature data logger ($\pm 3.5\%$ accuracy for RH and $\pm 1^\circ\text{C}$ accuracy for air temperature). The surface temperatures were measured using self-adhesive patch Type K thermocouples with miniature plugs; the measurements were collected using an Extech EA15 data-logging dual-input thermometer ($\pm 0.05\%$ of reading or $\pm 0.75^\circ\text{C}$, whichever is greater). The total incident solar radiation was measured using an Onset HOBO weather micro station with a pyranometer sensor ($\pm 10\text{ W/m}^2$ or $\pm 5\%$ accuracy, whichever is greater in sunlight). An Extech SDL310 thermo-anemometer with datalogging capability was used to collect the wind speed data 30 cm from the facade ($\pm 2\%$ reading $\pm 0.2\text{ m/s}$ accuracy). Wind speed measurements were made at a single point at the bare facade.

Table 1

Weather conditions during the experiments.

	8/29	8/30	8/31	9/1
Highest values				
Outdoor air temperature ($^\circ\text{C}$)	29.0	38.0	38.8	25.2
Relative humidity (%)	81	76	78	96
Wind speed (m/s)	0.40	2.20	2.00	0.90
Total horizontal solar radiation (W/m^2)	421	836	856	118
Average values				
Outdoor air temperature ($^\circ\text{C}$)	25.3	27.0	27.9	23.2
Relative humidity (%)	64	49	55	83
Wind speed (m/s)	0.06	0.22	0.14	0.02
Total horizontal solar radiation (W/m^2)	52	166	128	20
Lowest values				
Outdoor air temperature ($^\circ\text{C}$)	23.2	20.7	22.9	22.3
Relative humidity (%)	45	27	37	63
Wind speed (m/s)	0.05	0.00	0.00	0.00
Total horizontal solar radiation (W/m^2)	0	0	0	0

3.2. Experimental results and analysis

Three of the experimental days were mostly sunny; one day was cloudy. The measured data for the sunny days appeared very similar; therefore only a typical sunny day (August 31, 2013) was selected for analysis. The cloudy day was also selected for analysis (September 1, 2012). Table 2 and Fig. 4 show the average, maximum, and minimum values of the measured thermal properties of the two facade areas for each experimental day.

3.2.1. Surface temperatures

During full sun exposure, the bare facade exterior surface temperature reached as high as 41.5°C ; the difference between the facade and ambient air temperatures reached a maximum of 5.3°C .

Table 2

Measured thermal properties of the bare and vegetated facades.

Measured facade properties		8/29	8/30	8/31	9/1
Bare wall exterior surface temperature ($^\circ\text{C}$)	Max	33.7	40.6	41.5	26.2
	Ave	27.7	28.7	29.6	24.4
	Min	24.3	21.6	21.8	23.2
Vegetated wall exterior surface temperature ($^\circ\text{C}$)	Max	29.9	37.6	36.8	26.0
	Ave	26.1	27.5	28.6	24
	Min	24	21.6	22.2	23
Bare wall interior surface temperature ($^\circ\text{C}$)	Max	26.8	26.3	26.8	25.1
	Ave	25.6	24.1	24.9	22.9
	Min	23.2	22	21.9	21.8
Vegetated wall interior surface temperature ($^\circ\text{C}$)	Max	25.1	25.8	26.2	23.9
	Ave	24.1	23.5	24.2	22.1
	Min	22.2	21.6	21.2	21.3
Measured facade properties		8/29	8/30	8/31	9/1
Difference in exterior surface temperatures ($^\circ\text{C}$) (bare vs. vegetated wall)	Max	7.9	6.6	5.7	1.3
	Ave	1.6	1.2	1.1	0.4
Difference in interior surface temperatures ($^\circ\text{C}$) (bare vs. vegetated wall)	Max	2.0	1.1	1.7	1.3
	Ave	1.5	0.6	0.7	0.8
Difference in outside air temperatures ($^\circ\text{C}$) (bare vs. vegetated wall)	Max	2.9	4.0	3.3	0.5
	Ave	0.9	-0.5	-0.5	-0.3
Temperature difference between the exterior and interior wall surfaces (bare wall) ($^\circ\text{C}$)	Max	7.1	17.1	16.1	3.6
	Ave	2.04	4.65	4.77	1.48
Temperature difference between the exterior and interior wall surfaces (vegetated wall) ($^\circ\text{C}$)	Max	5.0	13.3	11.4	2.9
	Ave	1.97	3.98	4.41	1.84
Difference in wall temperature gradients ($^\circ\text{C}$) (bare vs. vegetated wall)	Max	6.1	6.2	5.5	0.9
	Ave	0.07	0.67	0.36	-0.35

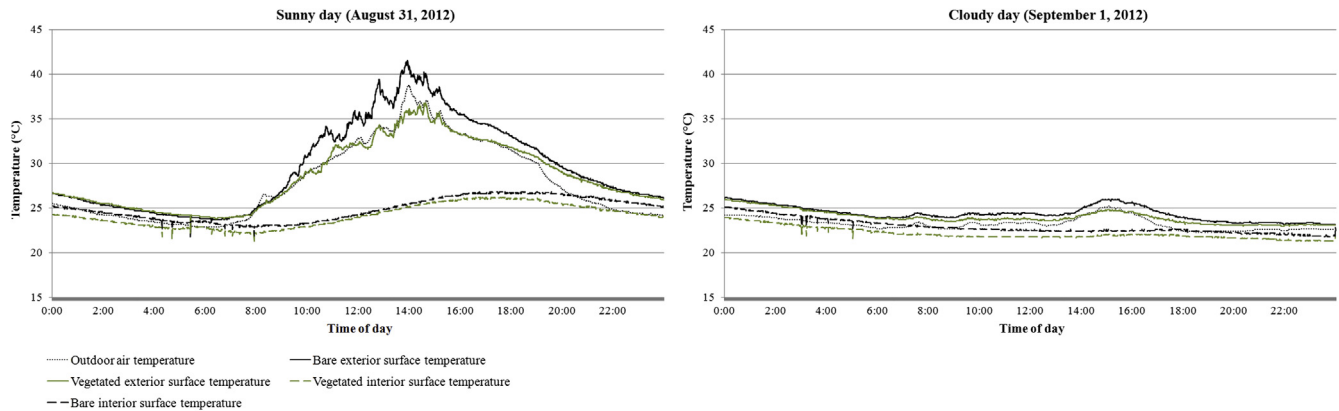


Fig. 4. Bare and vegetated facade temperatures measured on a sunny day (August 31, 2012) and a cloudy day (September 1, 2012).

At the same time, the vegetated facade exterior surface temperature typically closely matched the ambient air temperature and was never higher than 36.8 °C. The highest difference between the bare and vegetated exterior surface temperatures occurred around 14:00 (5.7 °C) and coincided with the highest values of solar radiation measured. This confirms that the most important plant effect is shading walls from solar radiation.

The average bare facade exterior surface temperature was 29.6 °C on the sunny and 24.2 °C on the cloudy day and the average vegetated facade exterior surface temperature was 28.6 °C on the sunny and 24 °C on the cloudy day. On the sunny day, the vegetated facade exterior surface temperature was consistently lower than that of the bare facade (mean difference of 1.1 °C), but it was approximately the same at night (Fig. 4). On the cloudy day, these two surface temperatures were closer throughout the day, but the exterior surface temperature behind plants was lower on average (mean difference of 0.4 °C) likely because plants absorbed diffuse solar radiation passing through the clouds.

The average interior surface temperature of the bare facade was 24.9 °C on the sunny day and 22.9 °C on the cloudy day, while that of the vegetated facade was 24.2 °C on the sunny day and 22.1 °C on the cloudy day. The interior surface temperature of the vegetated facade was always lower than that of the bare facade (mean difference of 0.9 °C). The peak interior surface temperature difference between the bare and vegetated facades occurred around 18:00, which did not correspond to the peak difference in the exterior surface temperatures. This can be explained by the thermal lag of the facade, which appears to be approximately 4 h for the 0.2 m thick masonry wall. Although not a focus of this study, it should be noted that this thermal lag effect can be beneficial for reducing cooling loads during peak hours in some climates even when peak solar radiation occurs several hours prior.

3.2.2. Temperature gradient (difference between the exterior and interior wall surfaces)

The measured temperature gradient from the exterior to interior surfaces served as a surrogate for heat conduction through the wall because the R -value of the wall itself is the same in both vegetated and bare cases. This gradient depended most strongly on changing exterior surface temperatures because they varied much more than interior surface temperatures did (indoors was inside a conditioned space). During sun exposure, the temperature gradient of the vegetated façade ($T_{svw} - T_{in}$) was consistently lower than that of the bare façade ($T_{sbw} - T_{in}$), with a mean of 4.4 °C and maximum of 11.4 °C compared to a mean 4.8 °C and a maximum of 16.1 °C. This difference, which depended on the time of day, suggests the vegetated layer can have significant energy benefits particularly

during times of direct sun exposure. At night and during the cloudy day, the temperature gradient of the vegetated facade was actually higher (mean 1.4 °C for the bare and 1.8 °C for the vegetated facades), presumably because its surface could not reject heat as effectively as the bare surface. However, the absolute difference was often low (i.e., <1 °C), meaning that conduction is not as important during these periods.

3.3. Model validation

These experimental results were used to validate the wall model by comparing the predicted and measured facade temperatures. Knowledge of the surface temperature reductions between the bare and vegetated facades allowed for estimation of other facade properties, such as a decrease in heat flux through the wall (assuming a constant R -value for the wall itself) and thus the instantaneous effective R -value of the plant layer. Several assumed plant and wall parameters were used in conjunction with the measured weather data (air temperature, solar radiation, relative humidity, and wind speed at the facade) as inputs in the model. Due to equipment limitations, the experiment measured only the global horizontal solar radiation, which was adjusted by modeling solar radiation on both a horizontal and a vertical surface using solar geometry for Chicago [29]. Correlations between the two surfaces were calculated and applied to the measured data to adjust the direct solar radiation data to a vertical surface. The validation was performed with the data for a sunny day (August 31, 2012) and a cloudy day (September 1, 2012).

The vegetation on the south facade consisted of a layer of mature Boston ivy (*Parthenocissus tricuspidata*). Several important plant characteristics were either assumed based on information from biophysics literature or directly measured, including:

- Leaf absorptivity coefficient: 0.5 (assumed).
- Average leaf dimension: 0.12 m (measured).
- Average leaf area index: 1.8 (measured).
- Radiation attenuation coefficient: 0.4 (assumed).
- Typical stomatal conductance: 0.2 mol/m² s (assumed).

The leaf absorptivity coefficient and the stomatal conductance values were adopted from the literature on biophysics and are considered appropriate for Boston ivy [14,15,25]. The average leaf dimension was found directly by measuring the width of several typical leaves in the plant layer. The radiation attenuation coefficient was found by visually evaluating a leaf angle of the plant layer. The leaf area index was estimated by measuring the area of a typical

leaf and counting the area of ivy leaves in an image of the vegetated facade under study.

The portion of the wall used in the experiment consisted of the two layers of cored brick with a small air gap in the middle and metal reinforcement elements, according to architectural drawings. Several assumptions for key facade parameters were made based on information on building materials in the literature [19,20].

- Wall thickness: 0.2 m (measured)
- Wall absorptivity: 0.7 for buff brick (assumed)
- Wall emissivity: 0.9 (assumed)
- Wall thermal resistance: 0.25 m² K/W (assumed)
- Wall density: 672 kg/m³ (assumed)
- Specific heat: 468 J/kg K (assumed)

The thermal resistance value of 0.25 m² K/W used for the validation was assumed to be lower than brick typical thermal resistance of 0.40 m² K/W [19] because of a combination of old facade construction, the likely abundance of metal elements in the wall composition, the large amount of poorly insulated windows and steel beams near our measured location, and the presence of large air cavities between the brick layers. The measured wall was composed of cored bricks where the total volume of solid brick material is estimated to be 60% based on details typical of the construction period (1940s). The remaining 40% of the wall volume is assumed to be air. Thus, with the assumed solid brick density of 1120 kg/m³, the actual wall density was estimated as approximately 60% of this number, or 672 kg/m³ [19]. Similarly, the actual wall specific heat was estimated as 60% of the assumed solid brick specific heat of 790 J/kg K, or 468 J/kg K.

Using the experimental weather conditions, the exterior surface temperatures for the bare (T_{sbw}) and vegetated facades (T_{svw}) were estimated at each one-minute time step using the model. Then, the differences between the exterior and interior wall surface temperatures of the bare ($T_{sbw} - T_{inbw}$) and vegetated ($T_{svw} - T_{invw}$) facades (i.e., temperature gradients through the brick layer) were calculated using the measured interior surface temperature (which remained near 24 °C in the air-conditioned space). The time-varying modeled values for exterior surface temperatures on the bare and vegetated wall for the sunny and cloudy day used in this work were first compared with the raw experimental data as shown in Fig. 5. Overall, the measured and modeled values for exterior surface temperatures on both the sunny and cloudy days were closely correlated. Coefficients of determination (R^2 values) between the measured and modeled facade surface temperatures for the bare and vegetated facades were 0.97 and 0.96 on the sunny day and 0.87 and 0.86 on the cloudy day, respectively.

The effective thermal resistance of the plant layer measured during the experiment varied throughout the day and reached a maximum of 0.14 m² K/W based on these measured values, which suggests that the plant layer reduced conductive heat transfer by as much as another ~10 cm layer of brick or ~0.5 cm of expanded polystyrene insulation in this particular climate and during these conditions [19,20]. Measured versus modeled correlations were generally lower for the facade temperature gradients than the surface temperatures alone, particularly for the cloudy day. Coefficients of determination (R^2 values) between the measured and modeled bare and vegetated facade temperature gradients were 0.96 and 0.92 on the sunny day and only 0.67 and 0.51 on the cloudy day, respectively. However, the variations in measured versus modeled facade surface temperatures and temperature gradients were small on the cloudy day for both facades and were generally within the uncertainty of both the facade surface temperature measurements (± 0.75 °C) and the facade temperature gradient measurements (estimated as ± 1.06 °C when added in quadrature), which suggests that the model successfully reproduced the measured results in all cases.

4. Discussion: sensitivity to weather and plant parameters

Using the validated model, the sensitivity of conductive heat transfer differences between the bare and vegetated facades ($Q_{bw} - Q_{vw}$) and the maximum plant instantaneous effective R -value (R_{plant}) to different weather parameters was analyzed. Heat flux was estimated using the interior-exterior surface temperature differences and constant thermal resistances for each facade. The sensitivity of multiple model parameters was explored by changing the values of one parameter at a time while keeping other parameters constant. Effects of the following inputs were evaluated: incident solar radiation, I_t (0 W/m², 400 W/m², and 800 W/m²); outdoor air temperature, T_{air} (15 °C, 20 °C, 25 °C, 30 °C, and 35 °C); relative humidity, RH (20%, 40%, 60%, 80%, and 100%); and wind speed, V_{air} (0.5 m/s, 1.5 m/s, 2.5 m/s, 3.5 m/s, and 4.5 m/s). The indoor temperature was assumed to be 24 °C in both cases. These parameter ranges represent an air-conditioned environment in warm weather conditions typical of plant growing seasons. The impact of each parameter is explored individually in the subsequent section. The model parameters that were held constant included a leaf absorptivity coefficient of 0.5; an average leaf dimension of 0.15 m; an average leaf area index of 2; a radiation attenuation coefficient of 0.5; a typical stomatal conductance of 0.2 mol/m² s; a wall thickness of 0.2 m; a wall absorptivity of 0.7; a wall emissivity of 0.9; a wall thermal resistance of 0.4 m² K/W; and

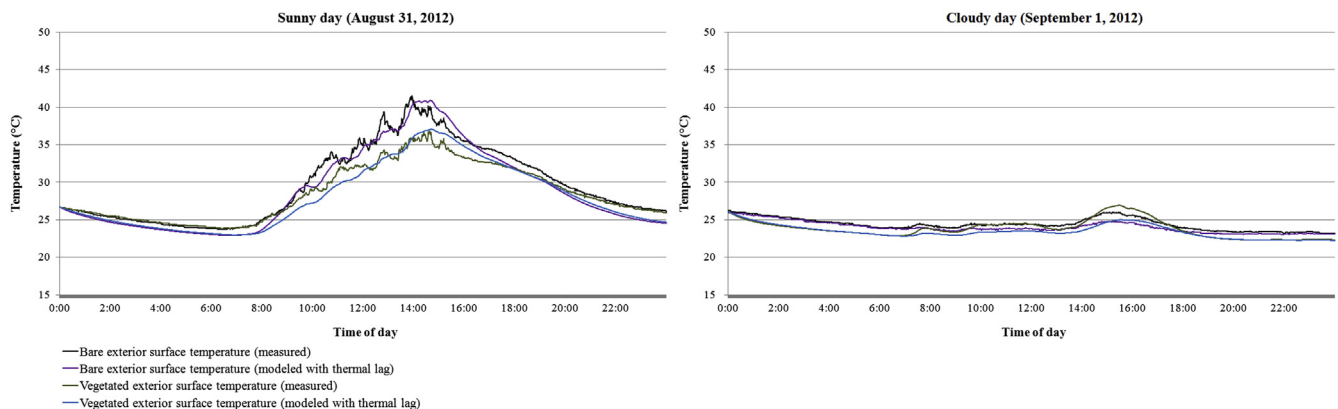


Fig. 5. Comparison of the measured and modeled exterior surface temperatures for the bare and vegetated facades on a sunny day (August 31, 2012) and a cloudy day (September 1, 2012).

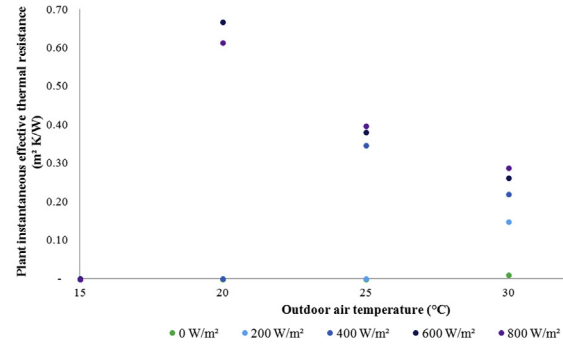
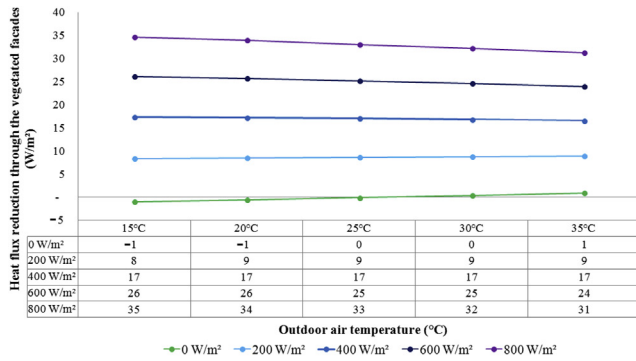


Fig. 6. Sensitivity of heat flux differences between the bare and vegetated facades (left) and plant effective thermal resistance (right) to incident solar radiation for relative humidity 50% and wind speed 1 m/s.

a heat capacity of 0 J/kg K. Figs. 6–8 summarize the results of the sensitivity analysis.

4.1. Sensitivity to incident solar radiation

Increasing solar radiation incident on the facade had the largest impact on the reduction in exterior surface temperature and heat flux through the bare and vegetated facades. Therefore, the positive effect of the vegetation cover and its effective thermal resistance increases significantly with incident solar radiation; that is, when the solar radiation level is the highest, the plant layer resistance is highest due to blocked transmission of radiation to the exterior wall surface. Conversely, when solar radiation is zero at night, the effective thermal resistance of the plant layer is negligible. For the range of solar radiation values explored (0–800 W/m² at RH = 50% and $V_{\text{air}} = 1$ m/s), the reduction in facade surface temperatures due to the plant layer ranged from 0 °C and 13.9 °C, corresponding to a heat flux reduction through the facade from 0 W/m² to 35 W/m². Similarly, the modeled effective plant R -value ranged from 0 m² K/W with no solar radiation to 0.67 m² K/W with the highest level of solar radiation. Therefore, the plant layer is shown to be particularly beneficial in climates and locations with high level of solar insolation. The plant layer is also particularly effective in cooling east and west facades that are exposed to the highest levels of solar radiation.

4.2. Sensitivity to outside air temperature

The modeled exterior facade surface temperatures and heat fluxes generally increased in response to increasing air temperatures. At higher air temperatures, the facade plant layer was

also less effective in cooling the facade exterior surface temperature and decreasing the heat flux through the facade. Concurrently, the effective thermal resistance of a plant layer gradually decreases when the air temperature rises. For the tested modeled range in air temperatures values between 15 °C and 35 °C (and with $I_t = 800$ W/m², RH = 50%, and $V_{\text{air}} = 1$ m/s), the reduction in facade surface temperatures due to the plant layer varied from 12.3 °C to 13.8 °C. Similarly, the heat flux reduction through the vegetated facade varied from 31 W/m² to 34 W/m², and effective plant R -values varied from 0 m² K/W to 0.22 m² K/W.

4.3. Sensitivity to relative humidity

For the modeled relative humidity values between 20% and 100% (with $I_t = 800$ W/m² and $V_{\text{air}} = 1$ m/s), the reduction in facade surface temperatures due to the plant layer ranged from 11.9 °C to 14.2 °C, heat flux reductions through the vegetated facade ranged from 30 W/m² to 36 W/m², and effective plant R -values ranged from 0.21 m² K/W to 0.67 m² K/W. When the relative humidity of air is low, plants significantly decrease the rate of evaporation as a way to protect themselves from drying out [15]. When the relative humidity is high, the rate of evaporation from plants greatly increases. This process is controlled by stomatal pores on the plant surface, which open and close depending on surrounding humidity. Because of this, a facade covered with the plant layer cools better at higher humidity levels. With increasing relative humidity, the exterior surface temperature reduction between the bare and vegetated facades increases and the plant effective thermal resistance increases as well, although the magnitude of effects is small relative to solar radiation and outdoor temperature.

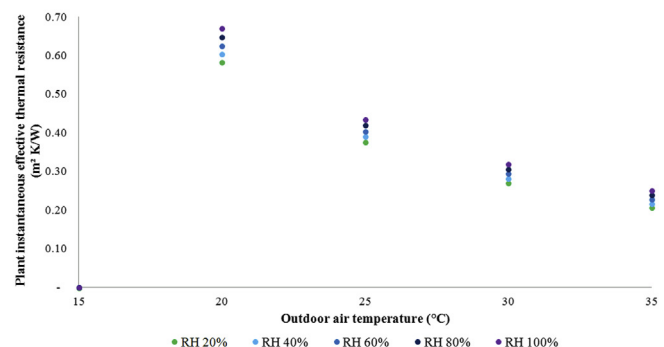
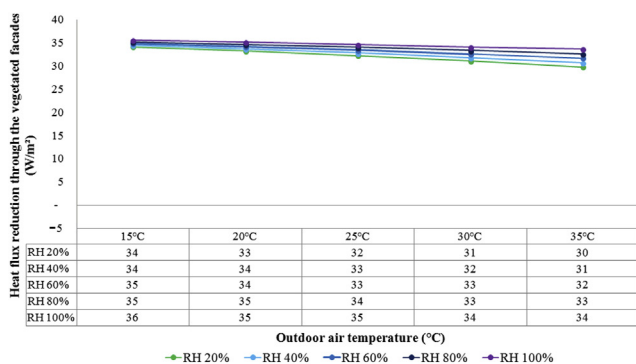


Fig. 7. Sensitivity of heat flux differences between the bare and vegetated facades (left) and plant effective thermal resistance (right) to relative humidity for solar radiation 800 W/m² and wind speed 1 m/s.

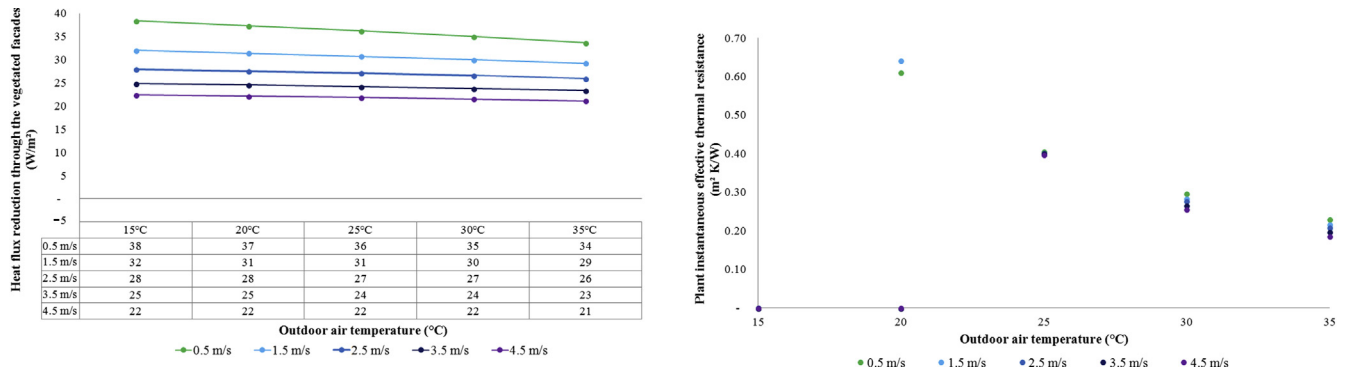


Fig. 8. Sensitivity of heat flux reductions between the bare and vegetated facades (left) and plant effective thermal resistance (right) to wind speed for solar radiation 800 W/m^2 and relative humidity 50%.

4.4. Sensitivity to wind speed

With increasing wind speed, the facade exterior surface temperature decreases as it cools more effectively due to convection. As a result, when the wind speed increases, the reduction in heat flux between the bare and vegetated facades and the effective plant R -value also decreases, although the modeled differences are small relative to the impacts of solar radiation. For the tested wind speed values between 0.5 m/s and 4.5 m/s (and with $I_t = 800 \text{ W/m}^2$ and $\text{RH} = 50\%$), the reduction in facade surface temperatures due to the plant layer ranged from 8.5°C to 15.4°C , heat flux reduction through the facade ranged from 21 W/m^2 to 39 W/m^2 , and effective plant R -value ranged from $0.19 \text{ m}^2 \text{ K/W}$ to $0.61 \text{ m}^2 \text{ K/W}$.

Overall, the heat flux reduction between the bare and vegetated facades and the plant effective thermal resistance are most sensitive to changes in solar radiation, followed by wind speed, relative humidity, and outdoor air temperature. The sensitivity analysis showed that adding a plant layer to a facade works best as a passive cooling strategy in climates with high solar radiation and low wind. The plant instantaneous effective R -value for the conditions used in the sensitivity analysis typically varied between 0.27 and $0.40 \text{ m}^2 \text{ K/W}$, with a maximum value of $0.71 \text{ m}^2 \text{ K/W}$, which suggests that a plant layer with the assumed characteristics could provide as much additional thermal resistance as $\sim 2.5 \text{ cm}$ of expanded polystyrene insulation. The effective plant R -values modeled in this study generally match plant layer thermal resistance values previously found in other studies, including Minke

[30] ($0.34 \text{ m}^2 \text{ K/W}$ for a 0.16 m thick ivy layer), Wong [12] ($0.36 \text{ m}^2 \text{ K/W}$ for a turf grass layer, $0.57 \text{ m}^2 \text{ K/W}$ for trees, and $1.61 \text{ m}^2 \text{ K/W}$ for shrubs), and Kontoleon and Evmorfopoulou [8] ($0.5 \text{ m}^2 \text{ K/W}$ for a 0.25 m thick ivy layer).

4.5. Sensitivity to plant parameters

The sensitivity analysis also evaluated the impacts of multiple plant parameters, including leaf area index (LAI), radiation attenuation coefficient (κ), leaf absorptivity (α_{leaf}), leaf typical dimension (D), and plant stomatal conductance (g_s). Among the evaluated parameters, only LAI and g_s were shown to have a significant effect on the plant layer thermal performance; therefore, this analysis is limited to calculating the vegetated facade properties with varying LAI and attenuation coefficient. Additionally, because solar radiation was shown to be the most important weather parameter in the previous sections, an extreme condition in a hot climate was chosen to compare the impacts of LAI and κ on the performance of the vegetated facade. A day in Phoenix, AZ with the highest solar radiation (June 10th according to TMY3 weather data) was chosen to explore the largest impact these plant parameters could likely have on reducing facade temperatures and thus heat flux through walls. The calculations were also performed for north, east, south, and west facades.

As we have shown, a layer of vegetation absorbs a fraction of incident solar radiation and transmits the rest through its foliage. The fraction of total absorbed radiation increases with higher

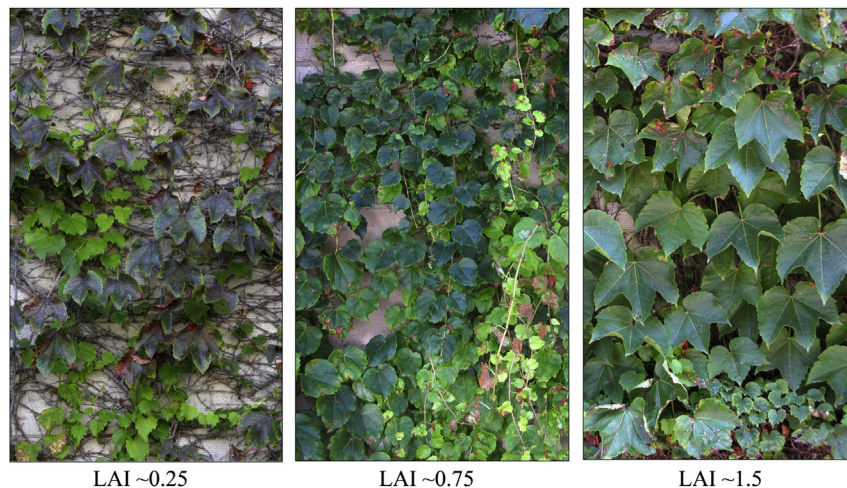


Fig. 9. Plant layer with different leaf area index.

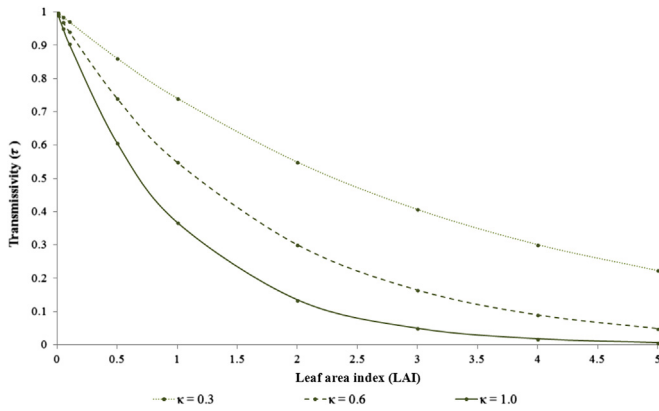


Fig. 10. Transmissivity coefficient depending on leaf area index and radiation attenuation coefficient.

vegetation density, which exponentially decreases the total radiation transmitted through a plant [25]. This attenuating effect is expressed through the radiation transmissivity coefficient τ , which is calculated with the widely used relationship developed by Monsi and Saeki in 1953 [13,28,31] as shown in Eq. (34).

$$\tau = \exp(-\kappa \text{LAI}) \quad (34)$$

where κ is the attenuation coefficient and LAI is a leaf area index. Fig. 9 shows examples of various LAIs of ivy walls and Fig. 10 shows the relationship between transmissivity, LAI, and κ .

With an increase in the leaf area index and attenuation coefficient, the facade temperature behind the vegetation and the heat flux through the wall decreases significantly because the plant layer with dense leaves oriented perpendicularly to the sun is most effective in blocking solar radiation incident on the wall (Fig. 11). Each unit increase in LAI resulted in an additional effective R -value of approximately $0.06 \text{ m}^2 \text{ K/W}$ on average, corresponding to a $\sim 5\%$ reduction in conductive heat transfer through the modeled wall per unit increase in LAI. There does appear to be a trend of somewhat diminishing returns with increasing LAI; however, we can conclude that a dense plant layer with a LAI of 3 or higher is particularly effective at cooling the exterior wall and reducing conductive heat transfer. For the modeled values of LAI between 0 and 4 (and assuming a constant $\kappa = 0.5$), the reduction in facade surface temperatures due to the plant layer varied between 0.8°C and 13.1°C ; the heat flux reduction between the facades ranged from 2 W/m^2 to 33 W/m^2 ; and effective plant R -values varied from $0.07 \text{ m}^2 \text{ K/W}$ to $0.50 \text{ m}^2 \text{ K/W}$, as shown in Fig. 11. For the modeled radiation attenuation coefficient values between 0 and 0.8

(assuming a constant $\text{LAI} = 2$, the reduction in facade surface temperatures due to the plant layer ranged from 0.7°C to 12.3°C ; the heat flux reduction between the facades ranged from 2 W/m^2 to 31 W/m^2 ; and effective plant R -value ranged from $0.06 \text{ m}^2 \text{ K/W}$ to $0.38 \text{ m}^2 \text{ K/W}$.

Overall, the analysis showed that a plant layer with densest foliage (high leaf area index) and with leaves parallel to the wall (high attenuation coefficient values) is the most successful in reducing facade surface temperatures and heat flux through the facade. These findings are in general agreement with the results of other experimental studies, which have shown a reduction in facade surface temperatures of $1.6\text{--}19^\circ \text{C}$ [8] and $6\text{--}11^\circ \text{C}$ [32] and reductions in facade heat flux of $4\text{--}11 \text{ W/m}^2$ [33] for vine-covered exterior walls.

Ultimately, the model developed and applied herein can be used to quantify the reduction in conductive heat load and its contribution to overall energy use for space conditioning in buildings with plant-covered facades. The model will help assess energy improvements in existing buildings retrofitted with green walls; it will also help design green walls for optimal energy efficiency in new construction. Additionally, this vegetated facade model can be used to form design guidelines for buildings with vegetated walls in various climates. Future model development should also include the effect of wind speed reduction due to a plant layer and more research should also be conducted on the role of a plant layer on air infiltration and general facade thermal performance in a cold climate.

5. Conclusion

A vegetated facade model has been developed to simulate the thermal effects of a building facade covered with a layer of plants. The developed mathematical model accounts for thermal and physical processes in a vegetated exterior wall including transmission of solar radiation through the vegetation layer, infrared radiative exchange between the facade and sky, the facade and ground, the facade and vegetation layer, convection to and from the facade, evapotranspiration from the plant layer, heat storage in the facade material, and heat conduction through the facade. The model was validated with results from a one-week long experiment that measured thermal properties of adjacent bare and vegetated facades on an existing building on the Illinois Institute of Technology campus. The experiment demonstrated that a plant layer on a facade can effectively reduce exterior surface temperatures on facades, daily temperature fluctuations indoors, exterior wall temperature gradients, and, as a result, heat flux through the exterior wall, particularly on days with high insolation. A sensitivity analysis showed that the most effective weather parameters

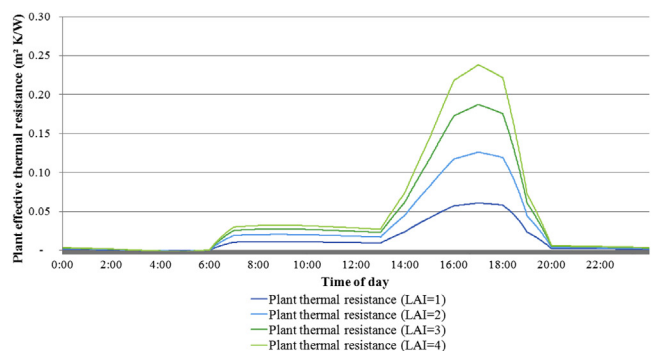
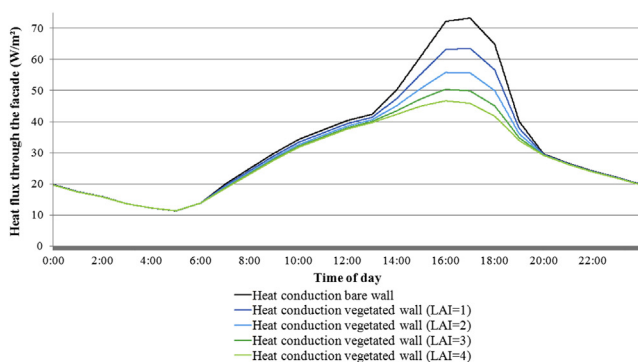


Fig. 11. Sensitivity of heat flux through the bare and vegetated facades (left) and plant effective thermal resistance (right) to leaf area index for a west facade in Phoenix on the brightest day ($\kappa = 0.5$).

include solar radiation, wind speed, relative humidity, and outdoor air temperature, in order of importance. The analysis also showed that plant layers with dense foliage (high leaf area indices) and with leaves parallel to the wall (high attenuation coefficients) are likely the most successful in reducing facade surface temperatures and heat flux through facades. On hot sunny days, a plant layer on a brick facade was estimated to reduce its exterior surface temperature by 0.7–13.1 °C, reduce the heat flux through the exterior wall by 2–33 W/m², and provide an effective *R*-value of 0.0–0.71 m² K/W, depending primarily on wall orientation, leaf area index, and radiation attenuation coefficient.

Acknowledgements

This research was conducted at the Illinois Institute of Technology and was funded by the Wanger Institute for Sustainable Research (WISER) Interdisciplinary Seed Funding Grant, 2011.

References

- [1] Hoyano A. Climatological uses of plants for solar control and the effects on the thermal environment of a building. *Energy and Buildings* 1988;11:181–99.
- [2] Di HF, Wang DN. Cooling effect of ivy on a wall. *Experimental Heat Transfer* 1999;235–45.
- [3] Evmorfopoulou EA, Kontoleon KJ. Experimental approach to the contribution of plant covered walls to the thermal behaviour of building envelopes. *Building and Environment* 2009;44:1024–38.
- [4] Wong NH, Kwang Tan AY, Chen Y, Sekar K, Tan PY, Chan D, et al. Thermal evaluation of vertical greenery systems for building walls. *Building and Environment* 2010;45:663–72.
- [5] Pérez G, Rincón L, Vila A, González JM, Cabeza LF. Green vertical systems for buildings as passive systems for energy savings. *Applied Energy* 2011;88:4854–9.
- [6] Perini K, Ottele M, Fraaij ALA, Haas EM, Raiteri R. Vertical gardening systems and the effect on air flow and temperature on building envelope. *Building and Environment* 2011;46:2287–94.
- [7] Holm D. Thermal improvement by means of leaf cover on external walls – a simulation model. *Energy and Buildings* 1989;14:19–30.
- [8] Kontoleon KJ, Evmorfopoulou EA. The effect of the orientation and proportion of a plant-covered wall layer on the thermal performance of a building zone. *Building and Environment* 2010;45:1287–303.
- [9] Alexandri E, Jones P. Developing a one-dimensional heat and mass transfer algorithm for describing the effect of green roofs on the built environment: comparison with experimental results. *Building and Environment* 2007;42:2835–49.
- [10] Sailor DJ. A green roof model for building energy simulation programs. *Energy and Buildings* 2008;40:1466–78.
- [11] Energy Plus engineering reference. United States Department of Energy; October 10, 2010.
- [12] Wong NH, Cheong DKW, Yan H, Soh J, Ong CL, Sia A. The effect of rooftop garden on energy consumption of a commercial building in Singapore. *Energy and Buildings* 2003;35:353–64.
- [13] Jones HG. Plants and microclimate. A quantitative approach to environmental plant physiology. Cambridge: Cambridge University Press; 1992.
- [14] Campbell GS, Norman JM. An introduction to environmental biophysics. New York: Springer; 1998.
- [15] Gates DM. Biophysical ecology. New York: Dover Publications, Inc; 2003.
- [16] Deardorff JW. Efficient prediction of ground surface temperature and moisture with inclusion of a layer of vegetation. *Journal of Geophysical Research* 1978;83:1889–903.
- [17] Zhang JQ, Fang XP, Zhang HX, Yang W, Zhu CC. A heat balance model for partially vegetated surfaces. *Infrared Physics and Technology* 1997;38:287–94.
- [18] Levitt J. Responses of plants to environmental stresses: chilling, freezing, and high temperature stresses. San Diego: Academic Press; 1980.
- [19] Larcher W. In: Physiological plant ecology. 4th ed. New York: Springer; 2003.
- [20] Straube J, Burnett E. Building science for building enclosures. Westford: Building Science Press Inc; 2005.
- [21] ASHRAE handbook fundamentals. Atlanta: American Society of Heating, Refrigerating and Air-Conditioning Engineers; 2009.
- [22] Asan H. Numerical computation of time lags and decrement factors for different building materials. *Building and Environment* 2006;41:615–20.
- [23] The R Project for Statistical Computing; March 13, 2013. Available from: <http://www.r-project.org/>.
- [24] Weather Data. United States Department of Energy; March 13, 2013. Available from: http://apps1.eere.energy.gov/buildings/energyplus/weatherdata_about.cfm?CFID=229916&CFTOKEN=b582a9b31f7c0ad9-CE02C17D-E418-423A-5F5546DCD5860F2C.
- [25] Monteith J, Unsworth M. In: Principles of environmental physics. 3rd ed. San Diego: Academic Press; 2007.
- [26] Nobel PS. Physicochemical and environmental plant physiology. Burlington: Academic Press; 2009.
- [27] Berdahl P, Martin M. Emissivity of clear skies. *Solar Energy* 1984;32:663–4.
- [28] Swinbank WC. Long wave radiation from clear skies. *Quarterly Journal of the Royal Meteorological Society* 1963;89:339–48.
- [29] Yu C. The intervention of plants in the conflicts between buildings and climate – a case study in Singapore. PhD thesis, National University of Singapore; 2006.
- [30] Pielke RA. Mesoscale meteorological modeling. San Diego: Academic Press; 2002.
- [31] Minke G, Witter G. Häuser Mit Grünem Pelz, Ein Handbuch zur Hausbe-grünung. Köln: Edition Fricke; 1985.
- [32] Hirose T. Development of the Monsi–Saeki theory on canopy structure and function. *Annals of Botany* 2005;95:483–94.
- [33] Price J. Green facade energetics. Master of Science thesis, University of Maryland; 2010.